



# Effect of Wet Spinning and Stretching to Enhance Mechanical Properties of Cellulose Nanofiber Filament

Hyun Chan Kim<sup>1</sup> · Debora Kim<sup>1</sup> · Ji Yun Lee<sup>1</sup> · Lindong Zhai<sup>1</sup> · Jaehwan Kim<sup>1</sup>

Received: 4 June 2018 / Revised: 6 August 2018 / Accepted: 13 August 2018 / Published online: 28 February 2019  
© The Author(s) 2019

## Abstract

Long filament made with nanocellulose has been researched due to its eminent mechanical and physical properties for next generation of natural fiber reinforced polymer composites. Wet spinning process for long filament fabrication in conjunction with stretching method has advantages of high efficiency and low-cost. To fabricate homogeneous and strong cellulose nanofiber filament, this paper experimentally investigates the process parameters, including spinning speed, pre-dry temperature and inner diameter of needle. In addition to the spinning process, a mechanical stretching process is taken into account to further improve the mechanical properties of the cellulose nanofiber filament. The effects of wet spinning and stretching are evaluated by using scanning electron microscope, tensile test and 2D wide angle X-ray diffraction. As a result, the stretched cellulose nanofiber filament exhibits its Young's modulus of 37.5 GPa and tensile strength of 543.1 MPa, which are significantly improved from the previous reports. All about the fabrication process, characterization and evaluation of the cellulose nanofiber filaments are illustrated.

**Keywords** Cellulose nanofiber · Filament · Wet spinning · Stretching · Mechanical properties

## 1 Introduction

Natural fiber reinforced polymer (NFRP) composites based on renewable resources have gained considerable interest from the industries due the environmental impact of their products. Those environmentally-friendly and low-cost NFRP composites can replace conventional materials such as glass fibers and synthetic plastics. Although advanced composites made with glass or carbon fibers have superior mechanical properties, they have critical issues in terms of

recycling and cost. To accomplish the concept of environmentally-friendly and low-cost NFRP composites, not only the fiber but also the resin polymer should be from natural resources. Thus, natural fibers and biodegradable polymers have become attractive recently.

Currently used natural fibers for NFRP composites are flax, hemp, jute, sisal, kenaf, coir, kapok, bamboo, banana, henequen and many others [1, 2]. Those natural fibers are commonly blended with resin polymers to form NFRP composites. However, mechanical properties of these blended NFRP composites are limited due to creep and stress relaxation of the composites. Thus, a bold departure of NFRP composites fabrication is essential by developing a high strength filament made with natural fibers to form a next generation of NFRP composite. Figure 1 shows the concept of the next generation of NFRP composite. This composite is reinforced with long filament of natural fibers in biodegradable polymer resins. The first step in this composite research is to develop a long filament made with natural fibers.

Cellulose is an almost inexhaustible raw polymer material with unique structure and properties. Since cellulose is biodegradable, renewable and biocompatible, it has many applications, not only paper, boards, laminates, additives, coatings, diapers and textiles but also the immobilization

---

✉ Jaehwan Kim  
jaehwan@inha.ac.kr  
Hyun Chan Kim  
Kim\_HyunChan@naver.com  
Debora Kim  
koi6020@hamail.com  
Ji Yun Lee  
sorodoro@naver.com  
Lindong Zhai  
duicaofei@naver.com

<sup>1</sup> Department of Mechanical Engineering, Creative Research Center for Nanocellulose Future Composites, Inha University, Incheon 22212, Republic of Korea

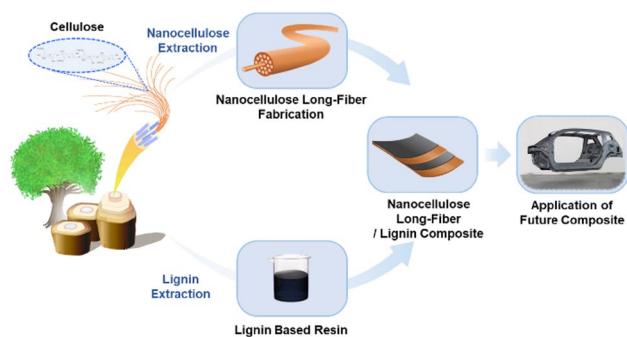


**Fig. 1** The new class of natural fiber reinforced polymer composite motivated from wood

of proteins and antibodies, optical films, pharmaceuticals and foodstuffs, as well as NFRP composites. Cellulose is broken down into nanocellulose composed of crystal parts and amorphous parts in a row. Crystal part in nanocellulose is called cellulose nanocrystal (CNC) meanwhile nanofibril composed of nanocellulose is named cellulose nanofiber (CNF). Nanocellulose has unique properties in terms of high mechanical strength and modulus, good optical transparency, low thermal expansion coefficient and thermally stable [3–5]. CNF has been studied as an important material for NFRP composites owing to its outstanding mechanical and physical properties, renewability, no industrial waste and energy saving by lightweight. However, its length is too short to form long filament [6]. Furthermore, mechanical properties of natural fibers are far less than those of nanocellulose. Once natural fibers are broken into CNFs, its mechanical properties can be increased by eliminating defects and impurities in natural fibers. Thus, it is essential to fabricate a long and strong filament by aligning CNFs, owing to its superior mechanical properties of CNF. To fabricate homogeneous CNF filament, a wet spinning process is an effective and low-cost method. In the wet spinning process, the filament of the raw polymer material is formed by the diffusional interchange between filament and coagulation solution [7]. In the previous researches, wet spun filaments were made from various raw materials such as graphene oxide [8], agar [9], polyvinylidene difluoride [10] and cellulose [11–15] in various kinds of coagulation solutions; acetone [11–13], ethanol [14], calcium chloride [15].

When CNF filament is formed, its strength can be greatly improved by aligning CNFs so as to make strong hydrogen bonds between CNFs. Beauty of the use of CNFs for strong CNF filament formation is that CNFs have abundant hydroxyl groups on their surfaces, such that they can form strong hydrogen bonds once they are well aligned together. Furthermore, since CNF is nano-size, its bonding sites are drastically increased comparing with micron-size pulp fibers in paper. By decreasing the size of CNFs and aligning them,

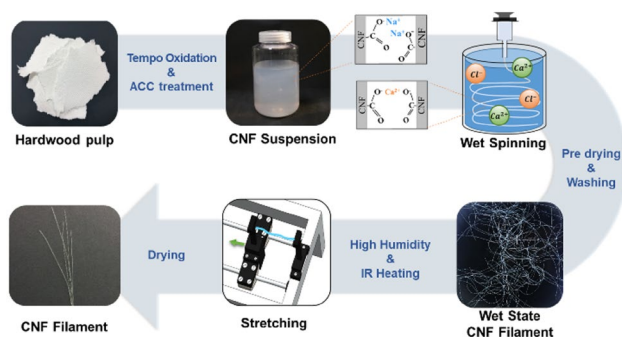


**Fig. 2** Schematic diagram of CNF filament fabrication process including CNF isolation, wet spinning and stretching processes

strong hydrogen bonds can be formed in the fabrication of strong and environmentally-friendly filament.

Besides, for better alignment of CNFs, additional processes can be used, for example, magnetic field [16], electric field [17] and hydrodynamics [18, 19]. However, they consume high energy and cost a lot for process setup compared with mechanical stretching. According to previous researches, various attempts of wet stretching were reported to form long filaments, including wet-stretching method progressed in wet solution [20], zone stretching method using two different roller speed ratio [21], cold drawing using tensile test machine at the room temperature [22] and simply physical stretching using shifting device [15]. In wet stretching, several parameters such as spinning speed, inner diameter of needle and dry temperature influence the results in terms of alignment of CNFs and hydrogen bonds between CNFs.

This work aims at fabricating a long and strong filament made with CNF by owing to its superior mechanical properties of nanocellulose. To achieve the goal, wet stretching parameters are investigated to enhance mechanical properties of the CNF filament. In addition, a stretching process is added to further improve the mechanical properties of the CNF filament. Figure 2 shows the schematic diagram of CNF filament fabrication process. The fabricated CNF filaments were characterized by scanning electron microscope (SEM), 2D wide angle X-ray diffraction (2DWAXD) and tensile test.

## 2 Experimental Method

### 2.1 Preparation of CNF Suspension

CNF can be isolated from various natural resources by means of chemical, physical and enzymatic methods [3]. Recently, a novel isolation method for CNF was reported, which uses the combination of a chemical method, TEMPO-oxidation

and a physical method, aqueous counter collision method [6]. The combined use of chemical and physical methods swells cellulose pulp and break CNFs apart from the pulp. In brief, hardwood pulp (30 g) was immersed in deionized (DI) water for 1 day. The swollen pulp was shredded by a food blender (LB-32HP, L'EQUIP), followed by a high-speed disperser (T25 digital, IKA). After adjusting the pulp suspension to 3 l by deionized (DI) water, a 2,2,6,6-tetramethylpiperidine-1-oxylradical (TEMPO, 0.375 g), sodium bromide (3.75 g) and sodium hypochlorite (600 ml) were mixed with the suspension for TEMPO-oxidation, while maintaining its pH to 12 using 0.5 M NaOH for 60 min. A pH meter (A211, Thermo Scientific) was used to monitor pH. After that, the pH was controlled to 7 by the adding 0.5 M HCl and the TEMPO reaction was finished by adding 10 ml ethanol. At the end of the reaction, chemically swollen cellulose macro fibers in the suspension were washed to remove remnant ions through a sieve (90  $\mu\text{m}$  pore size) with DI water. The washed cellulose macro fibers were pre-treated by using a homogenizer (UW 2200, BANDELIN) at 30 Hz, for 5 min. Pre-treated cellulose macro fibers were then physically isolated to CNFs by using an aqueous counter collision (ACC) machine (ACCNAC100, CNNT) with a pressure of 200 MP for 30 passes. Then, 1.7 wt% CNF suspension was obtained after the ACC treatment. At last, it was concentrated to 2 wt% CNF suspension through extraction of untreated cellulose macro fibers by means of ultra-centrifuge (CP80NX, HITACHI, Japan) at 40,000 rpm for 2 h.

## 2.2 Wet spinning

To fabricate CNF filaments, firstly, a wet-state CNF filament (WCF) was prepared by using the wet spinning with ion exchange [15]. The wet spinning process has three steps: coagulation, pre-drying and washing. At the coagulation step, the CNF suspension was extruded via a precision fluid dispenser (SMP3-C, MUSASHI Engineering) with different spinning speeds (580, 1160, 1700, 2300 cm/min) and different internal diameters of PTFE needle (380, 460, 560, 680, 960  $\mu\text{m}$ ) in 5 wt%  $\text{CaCl}_2$  solution baths for coagulation. The coagulated CNF suspension forms WCF and it was kept in the coagulation bath for 15 min. According to our previous study, the pre-drying step was made at 60  $^\circ\text{C}$  for 1 h to facilitate the hydrogen bond formation and ion linkage among CNFs with Calcium ion. In this study, we further investigated the effect of pre-drying temperature. At the pre-drying step, the WCF was stored in a convection oven and dried with various temperatures (30, 60, 90  $^\circ\text{C}$ ) for 30 min, which facilitates the hydrogen bond formation and ion linkage among CNFs with Calcium ion [23, 24]. Finally, at the washing step, the pre-dried WCF was immersed into DI water for 1 day so as to remove the non-reacted calcium ions and chloride ions on the WCF surface.

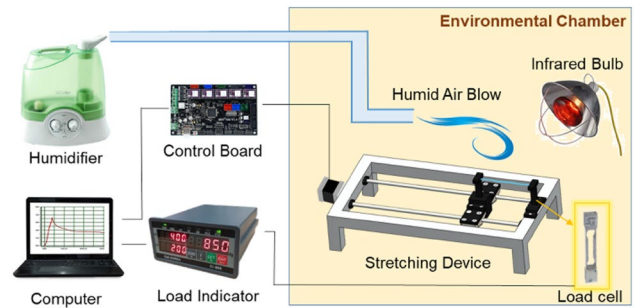


Fig. 3 Schematic diagram of stretching and drying process setup

For comparison, non-stretched CNF filament (NSCF) was fabricated by drying the WCF at room temperature for 1 day without stretching.

## 2.3 Stretching Process

Figure 3 shows the experimental setup for stretching and drying, composed of a stretching device, a control part and an environmental part. The stretching device consists of a linear guide fixed on an aluminum profile frame, a plastic fixture that holds one end of specimen, a plastic moving part that grabs the other end of specimen and moves along the linear guide by a timing belt, a timing pulley and a step motor (42BYGHN1641A series, Coact motor) that drives the timing belt, in turn produces linear movement of the plastic moving part.

The control part is composed of a loadcell (CB122 series, Dacell), a control board (MKS GEN V1.4, TEVO), an LCD display (LCD 2004, Bigtree tech), a load indicator (CI-100A, Cas Korea), a thermo-hygrometer (TH-05, Daekwang) and a computer. The control board is the main controller that sets up the Marlin firmware and is controlled by G-code. G-code commands to move the plastic moving part, by rotating the step motor through the timing belt, which stretches the wet CNF filament in 0.1 mm step. Two stretching ratios, 10% and 20% were assigned in the stretching experiment. To monitor the stretching process condition, the load cell was attached to the plastic fixture to look at the load condition. Throughout the stretching process, the load data was observed via the load indicator connected to the computer through RS232 serial communication port. Temperature and humidity data were observed by the thermo-hygrometer.

The environmental part is composed of an environmental chamber, two infrared heating bulbs, and a humidifier. Entire stretching and drying processes were carried out in the environmental chamber with temperature and humidity controlled. Two infrared heating bulbs (250 W) were installed to quickly dry up the wet CNF filament during the process. Although humidity was controlled by the environmental chamber, an additional humidifier (OSH-2081C,

Ohsung) was used to fully maintain the stretching condition in wet state. The stretching and drying experiment was carried out as follows. At first, the environmental chamber was set up to 24 °C and 90% RH. The humidifier was turned on to supply extra humidity to the specimen and kept 90% RH while stretching. Both sides of the specimen were securely clamped on the plastic fixture and the plastic moving part. The initial length was set to 60 mm. Next, the WCF specimen was stretched with two stretching ratios (10% and 20%). The stretching ratio was made by controlling the stretching distance by using G-Code on the controller. The G-code was programmed to make step movement of 0.1 mm in 1 s with 5 s pause. When the stretching was initiated, both heating bulbs were turned on at the same time to apply heat to the specimen gradually. Note that this experiment was performed in highly humid condition, 90% RH, not in a solvent or water. After the drawing process is finished, the humidifier was turned off and the environmental chamber door was opened to quickly drop the humidity to 20% RH. After the stretching and drying, stretched CNF filament (SCF) specimen was obtained and it was preserved in a desiccator with 20% RH for further test.

## 2.4 Characterization

The tensile test was carried out according to the standard (ASTM D-882-97) to estimate the mechanical properties of specimens in terms of Young's modulus, tensile strength, yield strength and strain at break. Each specimen was attached to a thin and transparent film using an Epoxy to make fixed ends on the specimen. The length of the specimens was 10 mm and the speed of the tensile test was set to 0.005 mm/s. Ten specimens were tested and averaged with different wet spinning parameters and stretching ratios.

2DWAXD of the fabricated SCF with different stretching ratios was measured using a high-performance X-ray diffractometer (D8 Discover, Bruker). CuK $\alpha$  radiation source at 50 kV and 1000  $\mu$ A was selected with a beam diameter of 0.3 mm in transmission mode for 300 s at 60 mm distance from the detector. Thirty filaments were bundled to get enough intensity.

## 3 Result and Discussion

To ascertain successful wet spinning in CaCl<sub>2</sub> coagulation solution, ion exchange effect was analyzed by energy dispersive X-ray spectroscopy (EDS) in scanning electron microscope (SEM, JSM-7100F, JEOL) as shown in Fig. 4. XPS Spectra appeared on Fig. 4a, b are from the CNF filament fabricated by the dry spinning and the wet spinning, respectively. The dry spinning specimen shows that sodium

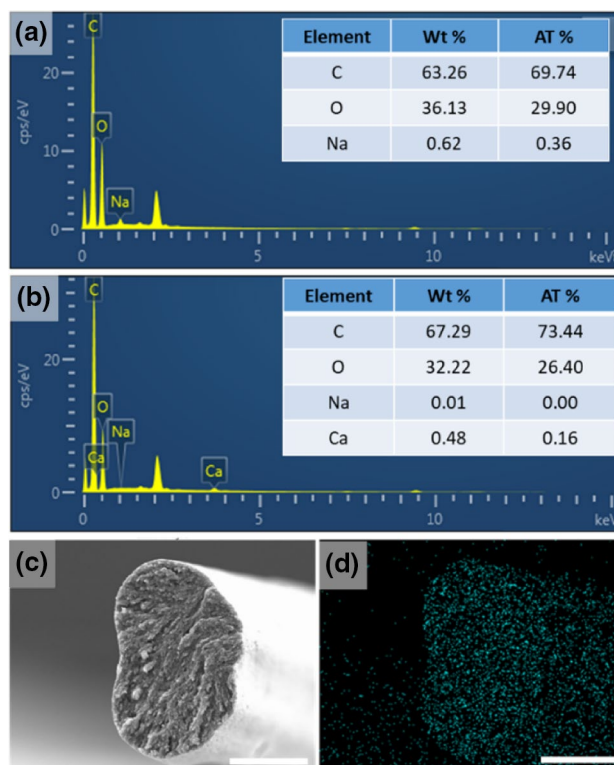


**Fig. 4** Result of SEM–EDS analysis. EDS spectrum of CNF filament fabricated **a** by air dry and **b** by wet spinning in CaCl<sub>2</sub> coagulation solution. **c** SEM cross-sectional image and **d** EDS mapping of elemental calcium (Ca). Scale bars are 25  $\mu$ m

ions are still remained in the filament meanwhile the wet spinning one exhibits no sodium ion but calcium ion instead. Figure 4c shows the cross-sectional SEM image of the CNF filament fabricated by the wet spinning and Fig. 4d represents its mapping of elemental calcium. The results reveal that the calcium ions in the coagulation solution substituted the sodium ions in CNF suspension and placed to the inside of the filament evenly. This indicates that the ion exchange was successfully performed, which results in enhancing ion interaction as well as hydrogen bond between CNFs.

To fabricate mechanically strong and tough CNF filament, the process parameters were investigated in terms of spinning speed, pre-dry temperature and inner diameter of spinning needle. Applying shear force on the CNF emulsion while flowing through the spinning needle is beneficial for aligning CNFs so as to improve mechanical properties. The spinning speed and inner diameter of needle are primary factors that govern shear stress inside of the needle. This shear stress can be expressed using the definition of Darcy's friction [25]:

$$\tau = \frac{1}{8} f_D \rho (v)^2, \quad (1)$$

where  $\tau$  is the shear stress,  $v$  is the spinning speed,  $\rho$  is the density and  $f_D$  is the friction factor. By using Hagen-Poiseuille equation, the friction factor can be found [26, 27] and the shear stress can be written as:

$$\tau = \frac{8\mu v}{d}, \quad (2)$$

where  $d$  is the inner diameter of needle,  $\mu$  is the viscosity of CNF emulsion. The shear stress is proportional to the spinning speed and inversely proportional to inner diameter of needle. Thus, the spinning speed and inner diameter of spinning needle are important parameters that influence the mechanical properties of CNF filament in the wet spinning process. In addition, pre-drying temperature is also an important parameter because it contributes to early stage hydrogen bonds among CNFs after the wet spinning. With increasing the pre-drying temperature, the formation of microbubbles is occurred quickly, at which they can be defectives in CNF filament [27].

Table 1 shows mechanical properties of the non-stretched CNF filaments (NSCF) in terms of Young's modulus, tensile strength, strain at break and yield strength obtained from the tensile test. At first, the spinning speed was varied by

550, 1160, 1700 and 2310 cm/min meanwhile the other parameters were fixed to arbitrary initial values. The case of 1700 cm/min exhibits the highest mechanical properties in terms of Young's modulus, tensile strength and yield strength except strain at break. As increasing the spinning speed, shear traction at the inside of the needle enhances the alignment of CNFs. However, over 1700 cm/min, the increased spinning speed rather deteriorates the alignment of CNFs due to excessive shear traction, which results in decreased mechanical properties. Notably, in comparison of 1700 cm/min with 550 cm/min, Young's modulus, tensile strength and yield strength increased to 48.4, 10.1 and 23.7%, respectively. For the pursuit of higher mechanical properties, the spinning speed was chosen to 1700 cm/min and other parameters were changed to optimize the process parameters. As the second parameter, the pre-dry temperature was tested by 30, 60 and 90 °C with the chosen spinning speed of 1700 cm/min. Above 100 °C, the CNFs in the suspension began denaturation with color change thus the temperature was changed below 100 °C [28]. In this experiment, the case of 30 °C reveals the highest mechanical properties. In comparison of 30 °C with 90 °C case, Young's modulus, tensile strength and yield strength increased to 43.6%,

**Table 1** Mechanical properties of non-stretched CNF filaments, NSCF, fabricated with different wet spinning parameters

Spinning speed change					
Spinning speed (cm/min)	550	1160	1700	2310	
Pre-dry temperature (°C)	60				
Needle inner dia. (μm)	960				
Stretching ratio (%)	0				
Young's modulus (GPa)	12.6±0.1	15.5±0.9	18.7±1.8	16.7±1.2	
Tensile strength (MPa)	246.6±8.3	245.9±26.3	271.4±36.0	266.3±11.7	
Strain at break (%)	11.7±1.2	7.4±1.0	7.4±2.1	9.9±2.6	
Yield strength (MPa)	63.6±5.0	64.3±14.5	78.7±12.7	75.9±10.2	
Pre-dry temperature change					
Spinning speed (cm/min)	1700				
Pre-dry temperature (°C)	30	60	90		
Needle inner dia. (μm)	960				
Stretching ratio (%)	0				
Young's modulus (GPa)	21.4±1.3	18.7±1.8	14.9±0.5		
Tensile strength (MPa)	366.8±22.5	271.4±36.0	237.8±15.2		
Strain at break (%)	5.5±0.7	7.4±2.1	10.4±0.6		
Yield strength (MPa)	141.3±17.1	75.1±12.6	54.1±8.2		
Inner diameter of needle change					
Spinning speed (cm/min)	1700				
Pre-dry temperature (°C)	30				
Needle inner dia. (μm)	380	460	560	680	960
Stretching ratio (%)	0				
Young's modulus (GPa)	24.3±2.9	24.2±2.7	23.3±2.2	23.0±0.8	21.4±1.3
Tensile strength (MPa)	492.6±22.1	472.2±17.8	403.5±29.5	370.7±31.7	366.8±22.5
Strain at break (%)	11.8±0.5	11.7±0.5	9.5±0.8	8.8±1.0	5.5±0.7
Yield strength (MPa)	291.0±32.5	247.6±11.3	202.2±43.6	190.3±7.2	141.3±17.1

54.2%, 161.2%, respectively. At the last parameter, the inner diameter of needle was changed to 380, 460, 560, 680 and 960  $\mu\text{m}$  with the flow speed of 1700 cm/min and the pre-dry temperature of 30 °C. The highest mechanical properties were observed when inner diameter of the spinning needle is 380  $\mu\text{m}$ . For comparison between 380  $\mu\text{m}$  and 960  $\mu\text{m}$ , Young's modulus, tensile strength and yield strength were improved by 13.6%, 34.3%, 105.9%, respectively.

Through the wet spinning parameter study, the optimal condition was found to be 1700 cm/min of flow rate, 30 °C of pre-dry temperature and 380  $\mu\text{m}$  of inner diameter of needle. To further improve the mechanical properties, the stretching was carried out by 10% and 20% of ratios with the optimal wet spinning condition. Table 2 shows the mechanical properties of SCF with the optimal wet spinning condition and the stretching ratio change. In comparison with NSCF, 20% SCF exhibits the largest Young's modulus, tensile strength and yield strength of 37.5 GPa, 543.1 MPa and 340.4 MPa, respectively. As the stretching ratio increased, CNFs in the filament aligned more so as to increase its Young's modulus and tensile strength. When these mechanical properties are compared with the initial parameter condition, its Young's modulus, tensile strength and yield strength are 2.98, 2.2 and 5.4 times increased, respectively.

Note that the stretching drastically improved Young's modulus, tensile strength and yield strength, meanwhile the strain at break was reduced by the stretching. Further study for improving the strain at break by stretching is future work.

Figure 5 shows SEM images of NSCF and 20% SCF, taken using field emission scanning electron microscope (S-4000, Hitachi). The 20% SCF has smoother surface than NSCF because CNFs are positioned closely and densely by improving the alignment of CNFs. Note that the diameter of CNF filament also decreased due to the stretching effect.

Figure 6a shows the azimuthal profiles of (200) diffraction in 2DWAXD of CNF. The intensity peak becomes narrow as the stretching ratio increases. Since the peak shape involves the orientation information of cellulose crystals in

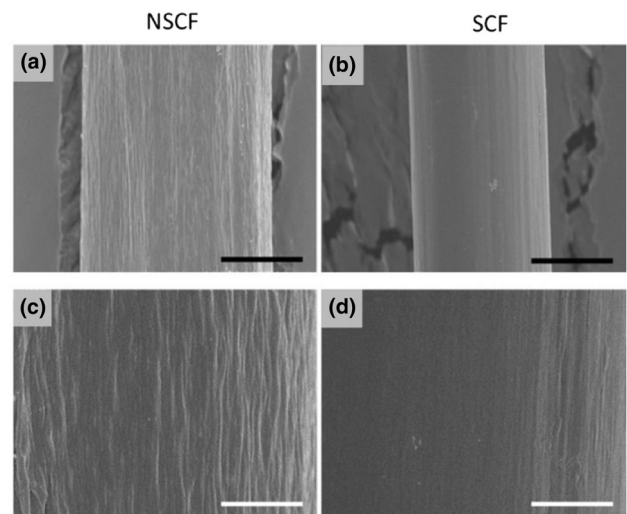


**Fig. 5** SEM images of NSCF (a, c) and SCF (b, d). Scale bars are 20  $\mu\text{m}$  for a and b, and 5  $\mu\text{m}$  for c and d

the fabricated filament, an orientation index ( $\alpha$ ) is calculated by the following equation in azimuthal breadth analysis:

$$\alpha = (180^\circ - \text{fwhm}) / 180^\circ. \quad (3)$$

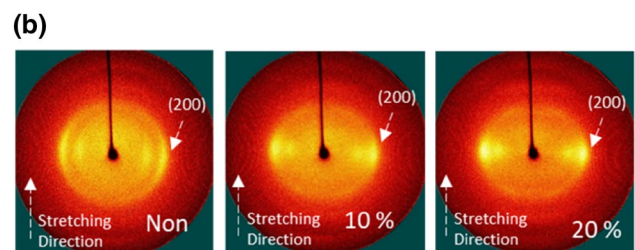
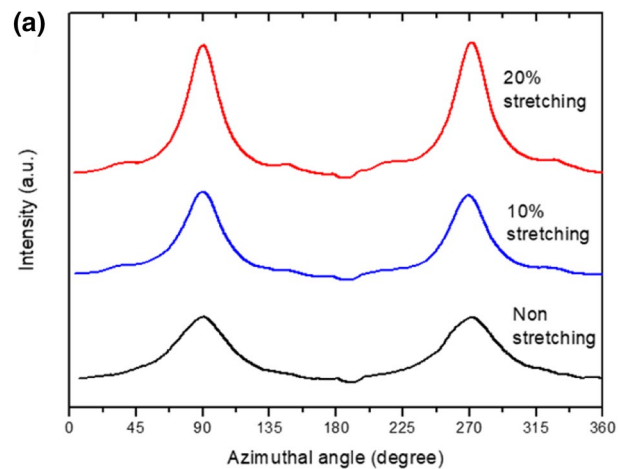


**Fig. 6** Result of 2DWAXD analysis with different stretching ratio. **a** Azimuthal profiles of (200) diffraction of CNF filament. **b** 2D diffraction pattern images with stretching direction

**Table 2** Mechanical properties of stretched CNF filaments, SCF, fabricated with the optimum wet spinning parameters with stretching ratio

Stretching ratio change			
Spinning speed (cm/min)	1700		
Pre-dry temperature (°C)	30		
Needle inner dia. ( $\mu\text{m}$ )	380		
Stretching ratio (%)	0	10	20
Young's modulus (GPa)	24.3 $\pm$ 2.9	31.8 $\pm$ 1.7	37.5 $\pm$ 1.6
Tensile strength (MPa)	492.6 $\pm$ 22.1	493.9 $\pm$ 16.6	543.1 $\pm$ 7.1
Strain at break (%)	11.8 $\pm$ 0.5	5.8 $\pm$ 0.8	3.7 $\pm$ 0.7
Yield strength (MPa)	291.0 $\pm$ 32.5	325.7 $\pm$ 21.1	340.4 $\pm$ 15.0
Orientation index	0.77	0.81	0.86

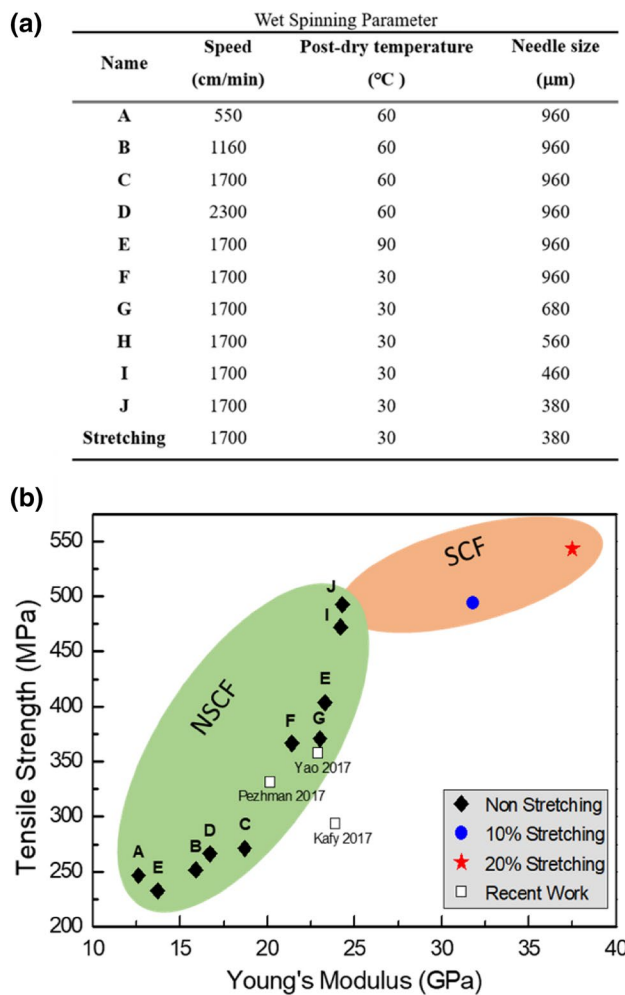


**Fig. 7** **a** List of wet spinning parameters experimented to compare the mechanical properties and **b** chart of tensile strength against Young's modulus with indicating range of mechanical properties of NSCF and SCF in comparison with references

Here, fwhm is the full width of the half maximum of the azimuthal profiles [20]. In the 2D diffraction pattern images shown in Fig. 6b, the intensity (200) plane appears clearly on the equator with the stretching ratio increase. It means that the SCF has improved CNF alignment along the stretching direction. The calculated orientation index is listed in the last row of Table 2. With increasing of the stretching ratio from 0 to 20%, the  $\alpha$ , increased by 17.0%.

In Fig. 7, the effect of wet spinning parameter and stretching process is summarized with index. The plotting of the tensile strength with respect to Young's modulus linearly increases. By controlling wet spinning parameters, Young's modulus increases from 12.6 to 24.3 GPa and tensile strengths does from 237.8 to 492.6 MPa. By stretching, Young's modulus and tensile strength are enhanced up to 37.5 GPa and 543.1 MPa, respectively.

These values show remarkable improvement comparing with recently reported Young's modulus and tensile strength values: 23.9 GPa and 294.1 MPa [15]; 20.17 GPa and 331 MPa [14]; 22.9 GPa and 357.5 MPa [13].

## 4 Conclusions

We investigated the effect of wet spinning and stretching process parameters to improve mechanical properties of environmentally-friendly filaments made with CNFs. For the base material, CNF suspension was isolated from hardwood pulp by using the combination of chemical and physical methods. The non-stretched CNF filaments were fabricated with wet spinning with various process parameters in terms of spinning speed, pre-dry temperature and inner diameter of needle. An optimal wet spinning condition was found by characterizing the non-stretched CNF filaments in terms of Young's modulus, tensile strength, yield strength and strain at break. In addition, the stretched CNF filaments were fabricated by drawing the wet-state CNF filament prepared from the optimal wet spinning condition. Finally, the 20% stretched CNF filament exhibited significantly enhanced mechanical properties (37.5 GPa of Young's modulus, 543.1 MPa of tensile strength and 340.4 MPa of yield strength) far better than the previously reported results. This remarkable improvement of mechanical properties of the stretched CNF filament is associated with the alignment of CNFs in the filament so as to increase hydrogen bonds between CNFs. The fabrication possibility of strong CNF filament is shown in this research by the low cost and simple methods. The fabricated environmentally-friendly filament will contribute to deliver the next generation of natural fiber reinforced polymer composites in real world.

**Acknowledgements** This study was supported by Creative Research Initiatives Program through the National Research Foundation of Korea (NRF) funded (NRF-2015R1A3A2066301).

**Open Access** This article is distributed under the terms of the Creative Commons Attribution 4.0 International License (<http://creativecommons.org/licenses/by/4.0/>), which permits unrestricted use, distribution, and reproduction in any medium, provided you give appropriate credit to the original author(s) and the source, provide a link to the Creative Commons license, and indicate if changes were made.

## References

- Lau, K.-T., Hunga, P.-Y., Zhu, M.-H., & Hui, D. (2018). Properties of natural fibre composites for structural engineering applications. *Composites Part B: Engineering*, 136, 222–233.
- Shah, A. U. R., Prabhakar, M., & Song, J.-I. (2017). Current advances in the fire retardancy of natural fiber and bio-based composites—A review. *International Journal of*

- Precision Engineering and Manufacturing-Green Technology*, 4(2), 247–262.
3. Kim, J. H., Shim, B. S., Kim, H. S., Lee, Y. J., Min, S. K., Jang, D., et al. (2015). Review of nanocellulose for sustainable future materials. *International Journal of Precision Engineering and Manufacturing-Green Technology*, 2(2), 197–213.
  4. Mahadeva, S. K., Kim, J., & Jo, C. (2011). Effect of hydrophobic ionic liquid loading on characteristics and electromechanical performance of cellulose. *International Journal of Precision Engineering and Manufacturing*, 12(1), 47–52.
  5. Kim, H. C., Mun, S., Ko, H. U., Zhai, L., Kafy, A., & Kim, J. (2016). Renewable smart materials. *Smart Materials and Structures*, 25(7), 073001.
  6. Hai, L. V., Zhai, L., Kim, H. C., Kim, J. W., Choi, E. S., & Kim, J. (2018). Cellulose nanofibers isolated by TEMPO-oxidation and aqueous counter collision methods. *Carbohydrate Polymers*, 191, 65–70.
  7. Paul, D. R. (1968). Diffusion during the coagulation step of wet-spinning. *Journal of Applied Polymer Science*, 12(3), 383–402.
  8. Cong, H. P., Ren, X. C., Wang, P., & Yu, S. H. (2012). Wet-spinning assembly of continuous, neat, and macroscopic graphene fibers. *Scientific Reports*, 2, 613.
  9. Liu, J., Xue, Z., Zhang, W., Yan, M., & Xia, Y. (2018). Preparation and properties of wet spun agar fibers. *Carbohydrate Polymers*, 181, 760–767.
  10. Jeong, K., Kim, D. H., Chung, Y. S., Hwang, S. K., Hwang, H. Y., & Kim, S. S. (2018). Effect of processing parameters of the continuous wet spinning system on the crystal phase of PVDF fibers. *Journal of Applied Polymer Science*, 135(3), 45712.
  11. Lundahl, M. J., Cunha, A. G., Rojo, E., Papageorgiou, A. C., Rautkari, L., Arboleda, J. C., et al. (2016). Strength and water interactions of cellulose i filaments wet-spun from cellulose nanofibril hydrogels. *Scientific Reports*, 6, 30695.
  12. Iwamoto, S., Isogai, A., & Iwata, T. (2011). Structure and mechanical properties of wet-spun fibers made from natural cellulose nanofibers. *Biomacromolecules*, 12(3), 831–836.
  13. Yao, J., Chen, S., Chen, Y., Wang, B., Pei, Q., & Wang, H. (2017). Macrofibers with high mechanical performance based on aligned bacterial cellulose nanofibers. *ACS Applied Materials & Interfaces*, 9(24), 20330–20339.
  14. Mohammadi, P., Toivonen, M. S., Ikkala, O., Wagermaier, W., & Linder, M. B. (2017). Aligning cellulose nanofibril dispersions for tougher fibers. *Scientific Reports*, 7, 11860.
  15. Kafy, A., Kim, H. C., Zhai, L., Kim, J. W., Kang, T. J., & Kim, J. (2017). Cellulose long fibers fabricated from cellulose nanofibers and its strong and tough characteristics. *Scientific Reports*, 7, 17683.
  16. Kim, J., Chen, Y., Kang, K. S., Park, Y. B., & Schwartz, M. (2008). Magnetic field effect for cellulose nanofiber alignment. *Journal of Applied Physics*, 104, 096104.
  17. Bordel, D., Putaux, J. L., & Heux, L. (2006). Orientation of native cellulose in an electric field. *Langmuir*, 22(11), 4899–4901.
  18. Håkansson, K. M. O., Fall, A. B., Lundell, F., Yu, S., Krywka, C., Roth, S. V., et al. (2014). Hydrodynamic alignment and assembly of nanofibrils resulting in strong cellulose filaments. *Nature Communications*, 5, 4018.
  19. Mittal, N., Jansson, R., Widhe, M., Benselfelt, T., Håkansson, K. M., Lundell, F., et al. (2017). Ultrastrong and bioactive nanostructured bio-based composites. *ACS Nano*, 11(5), 5148–5159.
  20. Torres-Rendon, J. G., Schacher, F. H., Ifuku, S., & Walther, A. (2014). Mechanical performance of macrofibers of cellulose and chitin nanofibrils aligned by wet-stretching: A critical comparison. *Biomacromolecules*, 15(7), 2709–2717.
  21. Yun, S., & Kim, J. (2010). Evaluation of cellulose electroactive paper made by tape casting and zone stretching methods. *International Journal of Precision Engineering and Manufacturing*, 11(6), 987–990.
  22. Sehaqui, H., Mushi, N. E., Morimune, S., Salajkova, M., Nishino, T., & Berglund, L. A. (2012). Cellulose nanofiber orientation in nanopaper and nanocomposites by cold drawing. *ACS Applied Materials & Interfaces*, 4(2), 1043–1049.
  23. Peng, Y., Gardner, D. J., & Han, Y. (2012). Drying cellulose nanofibrils: in search of a suitable method. *Cellulose*, 19(1), 91–102.
  24. Sone, A., Saito, T., & Isogai, A. (2016). Preparation of aqueous dispersions of TEMPO-oxidized cellulose nanofibrils with various metal counterions and their super deodorant performances. *ACS Macro Letters*, 5(12), 1402–1405.
  25. Chaudhry, M. H. (2014). *Applied hydraulic transients* (3rd ed., p. 45). New York: Springer.
  26. Lundahl, M. J., Klar, V., Wang, L., Ago, M., & Rojas, O. J. (2016). Spinning of cellulose nanofibrils into filaments: A review. *Industrial and Engineering Chemistry Research*, 56(1), 8–19.
  27. Romeo, E., Royo, C., & Monzon, A. (2002). Improved explicit equations for estimation of the friction factor in rough and smooth pipes. *Chemical Engineering Journal*, 86(3), 369–374.
  28. Matsuo, M., Umemura, K., & Kawai, S. (2012). Kinetic analysis of color changes in cellulose during heat treatment. *Journal of Wood Science*, 58(2), 113–119.

**Publisher's Note** Springer Nature remains neutral with regard to jurisdictional claims in published maps and institutional affiliations.



**Hyun Chan Kim** Ph.D. candidate in the Department of Mechanical Engineering, Inha University. His research interest is nanocellulose, sensor and actuator, microfabrication.



**Debora Kim** M.S. student in the Department of Mechanical Engineering, Inha University. His research interest is nanocellulose and composite material.





**Ji Yun Lee** M.S. student in the Department of Mechanical Engineering, Inha University. His research interest is nanocellulose and design process.



**Jaehwan Kim** Professor in the Department of Mechanical Engineering, Inha University. His research interest is cellulose, smart materials, structure and devices, electroactive polymers and smart sensors.



**Lindong Zhai** Ph.D. candidate in the Department of Mechanical Engineering, Inha University. His research interest is cellulose EAPap, ACC, nanocellulose, piezoelectric and AFM.